ARMY RESEARCH LABORATORY

Cycle Life Enhancement in Cu-Sn Anodes

Jeff Wolfenstine, Donald Foster, Jeffrey Read, and Wishvender Behl

ARL-TR-2664 May 2002

The findings in this report are not to be construed as an official Department of the Army position unless so designated by other authorized documents.

Citation of manufacturer's or trade names does not constitute an official endorsement or approval of the use thereof.

Destroy this report when it is no longer needed. Do not return it to the originator.

Army Research Laboratory

Adelphi, MD 20783-1197

ARL-TR-2664 **May 2002**

Cycle Life Enhancement in Cu-Sn Anodes

Jeff Wolfenstine, Donald Foster, Jeffrey Read, and Wishvender Behl

Sensors and Electron Devices Directorate

Abstract

This technical report summarizes the work on two different approaches that have been used to increase the cycle life of active-inactive composites in the copper-tin system. The first approach is to reduce the particle size of the active-inactive composities to the nano-scale (<100 nm). The second approach is the addition of extra elements that segregate to grain/phase boundaries and increase the cohesive strength of the boundary. Both approaches significantly improved the capacity retention of a Cu6Sn5 alloy. A larger improvement in capacity retention was exhibited by the addition of 10-wt.% iron compared to the reduction of the particle size to the nano-scale. The volumetric capacity of the Cu6Sn5 alloy containing 10 wt.% iron at 100 cycles is almost three times the theoretical capacity of graphite. The Cu6Sn5-10 wt.% Fe material has potential as a replacement anode for graphite in lithium-ion batteries.

Contents

Figures

Introduction

Recently, there has been interest in the use of composites consisting of a lithium active metal (metal that alloys with lithium (Li), i.e., tin (Sn)) dispersed within an inactive matrix (i.e., copper (Cu)) as replacement anodes for graphite in Li-ion batteries [**1–15**]. Active-inactive composites are preferred over an anode consisting only of a lithium alloy, even though there is loss of specific capacity because of the extra weight of the inactive component because the cycle life of the alloy is very limited. Dispersing the alloy within a matrix reduces the mechanical stresses associated with Li insertion/removal during charging/discharging and thus improves the cycle life compared to the alloy alone. However, active-inactive composites still suffer from a restricted cycle life that limits their use in commercial and military applications. Thus, there is a need to develop ways to improve the cycle life of active-inactive composites so they can be used in practical applications.

This technical report summarizes the work on two different approaches that have been used to increase the cycle life of active-inactive composites in the copper-tin (Cu-Sn) system. The first approach is to reduce the particle size of the active-inactive composites to the nano-scale (<100 nm). The second approach, which has not attracted much attention in the battery community but is used in structural materials to improve the fracture toughness of the material, is the addition of extra elements, particularly elements that segregate to grain/phase boundaries and increase the cohesive strength of the boundary and thus, its resistance to fracture [**16–21**]. The results of both approaches will be compared to 1) graphite and 2) copper-tin active-inactive composites with micron-sized particles.

Material Selection

For this investigation, the Cu_6Sn_5 alloy in the Cu-Sn system was chosen for the following reasons: 1) It has been shown that as Li is added to Cu_6Sn_5, it eventually decomposes to a Li-Sn alloy (active) surrounded by a Cu matrix (inactive) (i.e., forms active-inactive composite) [**11–14**]; 2) The volumetric capacity of a Cu_6Sn_5 alloy made by conventional melting [**12**] at 10 cycles was about twice the capacity for graphite, whereas for the Cu_6Sn_5 alloy at 25 cycles made by mechanical alloying [**14**], the capacity was about three times that for graphite. Thus, Cu_6Sn_5 has potential as a replacement for graphite in Li-ion batteries if its cycle life can improved; and 3) there is experimental evidence for the Cu_6Sn_5 alloy in the micron-size particle range that as the particle size is decreased, an improvement in cycle life is exhibited [**15**].

Experimental

Nano-scale Cu_6Sn_5 powders were synthesized by a chemical method, which involved reducing a methanol solution of copper chloride ($CuCl_2$) and tin chloride ($SnCl_2$) (1.2:1 volume ratio) with sodium tetrahydridoborate ($NaBH_4$) in a 14 Molar sodium hydroxide (NaOH) solution under constant stirring at room temperature. Twice the amount of the $NaBH_4$ solution was added to the methanol solution containing the Cu and Sn ions to ensure complete reduction of the metal ions. Upon addition of the $NaBH_4$ solution, a black precipitate was observed immediately. The black precipitate was washed with distilled water and filtered until the pH of the filtrate was the same as that of the distilled water. The precipitate was then dried at 100° C under vacuum.

The second approach involved the addition of a third element, Fe, to a Cu_6Sn_5 alloy. Iron was chosen as the additional element for the following reasons: 1) It has been shown theoretically based on a first-principles approach that Fe will segregate to grain boundaries in Ni_3Al and will enhance the room temperature cohesive strength of the boundaries [**20**]; 2) It has been shown that Fe additions to a Zn-22 wt.% Al alloy [**21–23**] segregated to grain boundaries and made these boundaries more resistant to sliding at elevated temperature. It was anticipated that Fe would segregate to grain boundaries in the Cu_6Sn_5 alloy and would increase their resistance to fracture and thus improve cycle life.

The material investigated in this study was Cu_6Sn_5+10 wt.% Fe. Elemental powders of Cu, Sn, and Fe in the correct ratio to form a Cu_6Sn_5+10 wt.% Fe material were placed in a hardened steel jar along with several steel balls under an argon atmosphere containing less than 1 ppm of oxygen and water. The jars were shaken with a Spex mixer mill for 20 hours. After milling, the powders were cold pressed into pellets in a glove box under an argon atmosphere containing less than 1 ppm oxygen and water. The pellets were melted in a molybdenum (Mo) crucible in the glove box at 1100° C for about 24 hours, after which, the liquid was quickly poured onto a stainless steel pain to rapidly cool it. The quenched material was crushed, ground, and sieved to less than 45 μm.

Powders from both approaches were characterized by x-ray diffraction, scanning electron microscopy (SEM), and transmission electron microscopy (TEM). Powders for TEM were prepared by dispersing them in methanol, and while they were in an ultrasonic bath, a drop of the suspension was placed on a nickel grid covered with an amorphous carbon film.

The cycle life of the Cu_6Sn_5 powders was evaluated in half cells at room temperature. Cu_6Sn_5 positive electrodes were prepared by mixing 85-wt. % alloy powders, 5-wt.% carbon, and 10-wt.% polyvinylidene fluoride dissolved in N-methylpyrrolidinone. The mixture was coated onto a Cu substrate. The electrodes were dried under vacuum. Metallic lithium was used as the negative electrode. The electrolyte solution was 1 Molar Lithium Hexafluorophosphate:Ethlylene Carbonate/ Dimethyl Carbonate/Diethyl Carbonate (5:4:1 by volume). The cells were cycled at a constant current density of 0.1 mA/cm^2 between 0.0 to 1.0 V. After cycling, the structure of the alloys was investigated with x-ray diffraction.

Results and Discussion

Figure 1 is an x-ray diffraction pattern of the Cu_6Sn_5 powders after precipitation. From Figure 1, it can be observed that the precipitate was single-phase Cu_6Sn_5. No other Cu-Sn phases or pure component (Cu or Sn) peaks were exhibited in the x-ray diffraction pattern. The average crystallite size calculated with the Scherrrer formula [**25**] was 10 nm. X-ray microanalysis on particles that were cold mounted and polished revealed that the Cu and Sn were uniformly distributed with a Cu:Sn of about 1:1, which is in good agreement with the desired Cu:Sn of 1.2:1 for the Cu_6Sn_5 alloy. SEM analysis revealed that the particles exhibited an equiaxed morphology, with all particles less than 100 nm. The average particle size determined with the line intercept method [**26**] on more than 200 particles was estimated to be about 40 nm. TEM confirmed that all particles were nano-scale (<100 nm). Figure 2 is a TEM photomicrograph of some nano-scale Cu_6Sn_5 powders. It shows equiaxed particles with a size between 30 and 40 nm.

The x-ray diffraction pattern for the Cu_6Sn_5+10 wt.% Fe material revealed mainly peaks corresponding to Cu_6Sn_5 and to a lesser extent, those for elemental Fe. No other Cu-Sn, Cu, Sn, or Cu-Fe peaks were observed. Some very small peaks corresponding to FeSn and $FeSn_2$ were observed. However, they were very much smaller than those for elemental Fe. From the x-ray diffraction data, it was concluded that the material is mostly single-phase Cu_6Sn_5 with elemental Fe as a second phase. X-ray microanalysis with the SEM on particles that were cold mounted and polished

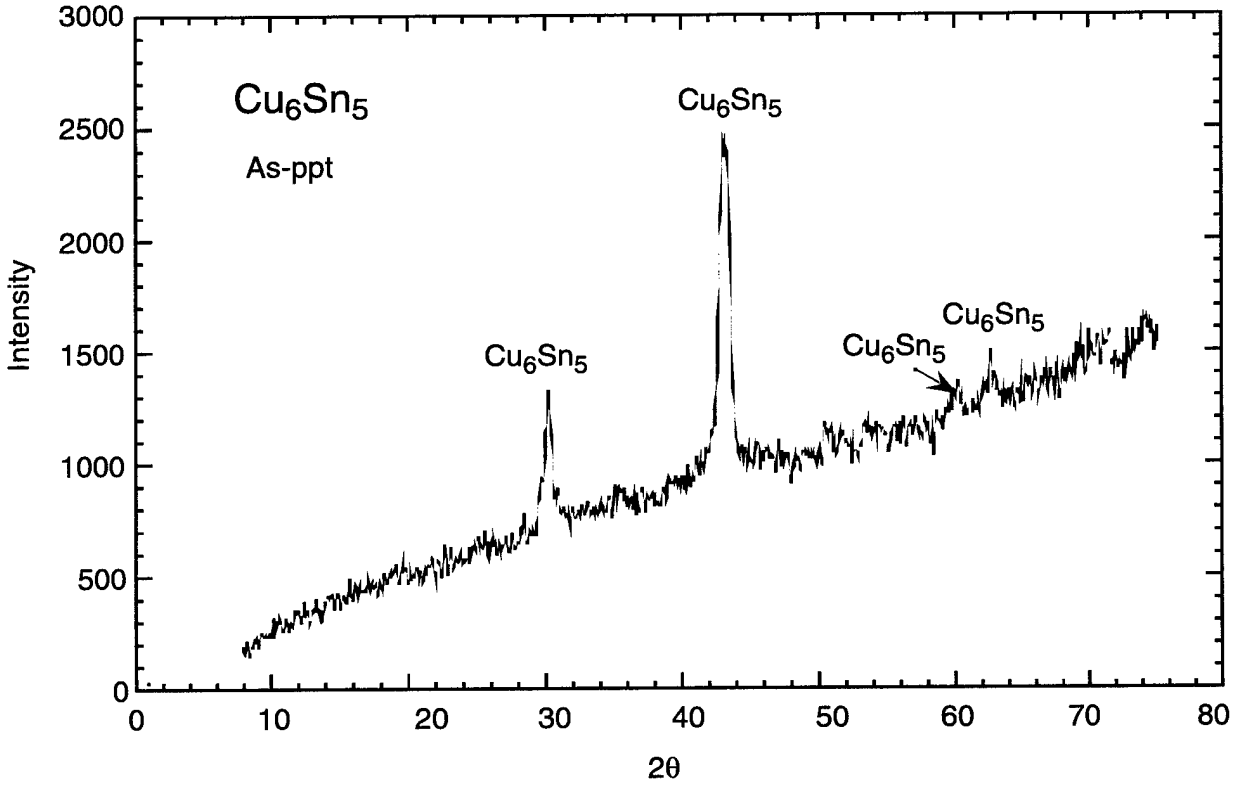

Figure 1. X-ray Diffraction Pattern of the As-precipitated Material.

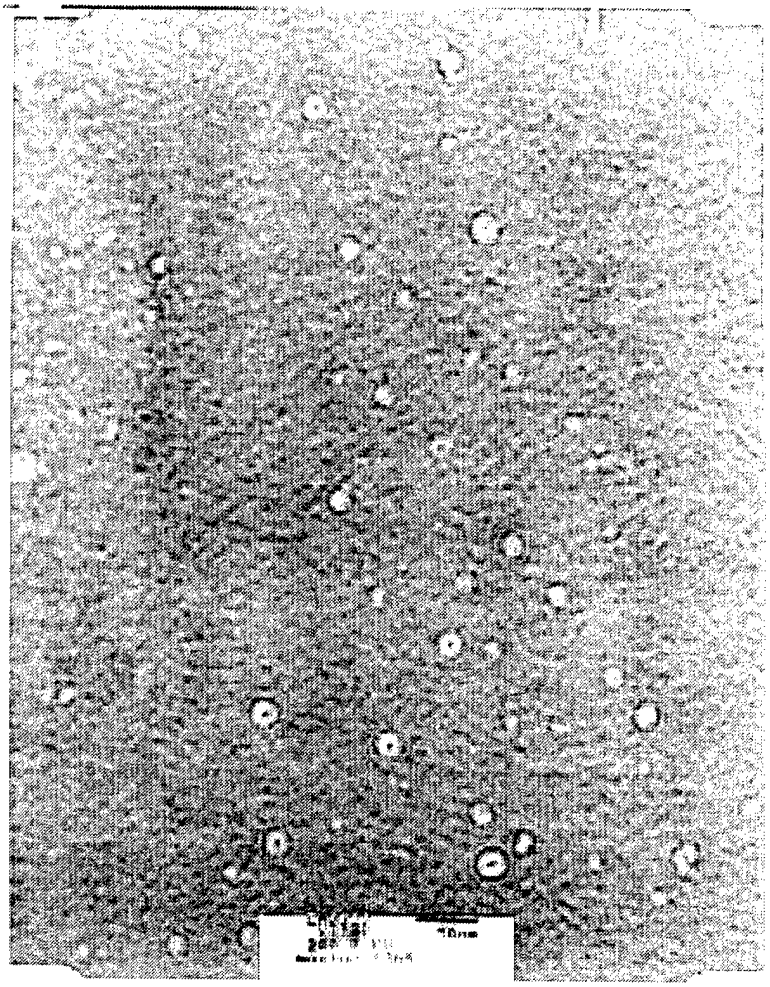

Figure 2. Transmission Electron Photomicrograph of Some Nano-scale Cu_6Sn_5 Powders.

revealed that the Cu and Sn were uniformly distributed with a Cu:Sn ratio of about 1.1:1, which is in excellent agreement with the desired Cu:Sn of 1.2:1 for the Cu_6Sn_5 alloy. Iron was observed to be non-uniformily distributed. X-ray microanalysis revealed that the volume fraction of Fe converted to a wt.% was about 8% to 9%, which is in good agreement with the desired 10 wt.%. The average particle size of the Cu_6Sn_5+10 wt.% Fe material was about 6 μm. Preliminary TEM x-ray microanalysis confirmed a non-uniform Fe distribution within the particles. However, at present, it is not possible to specify the Fe location (i.e., along grain boundaries).

The volumetric capacity of the nano-scale Cu_6Sn_5 alloy (≈ 40 nm) (Approach 1) Cu_6Sn_5+10 wt.% Fe material (Approach 2) versus cycle number are plotted in Figure 3. Also shown in Figure 3 are data for graphite (theoretical capacity) [**11**] and the Cu_6Sn_5 alloy with micron-sized particles (information about the particle size is listed in parentheses) prepared by conventional melting (< 38 μm) [**12**] and mechanical alloying (<1 μm) [**14**]. From Figure 3, several important points are noted. First, it can be observed that the extrapolated capacity approaches zero at about 45 to 50 cycles for the melted alloy and 80 to 85 cycles for the mechanical alloyed material. In contrast, at 100 cycles, the nano-scale Cu_6Sn_5 and Cu_6Sn_5+10 wt.% Fe material powders still have a significant amount of reversible capacity. This result shows that both approaches (nano-scale and Fe addition) have significantly improved the capacity retention of the Cu_6Sn_5 alloy. Second, the capacity of the Cu_6Sn_5-

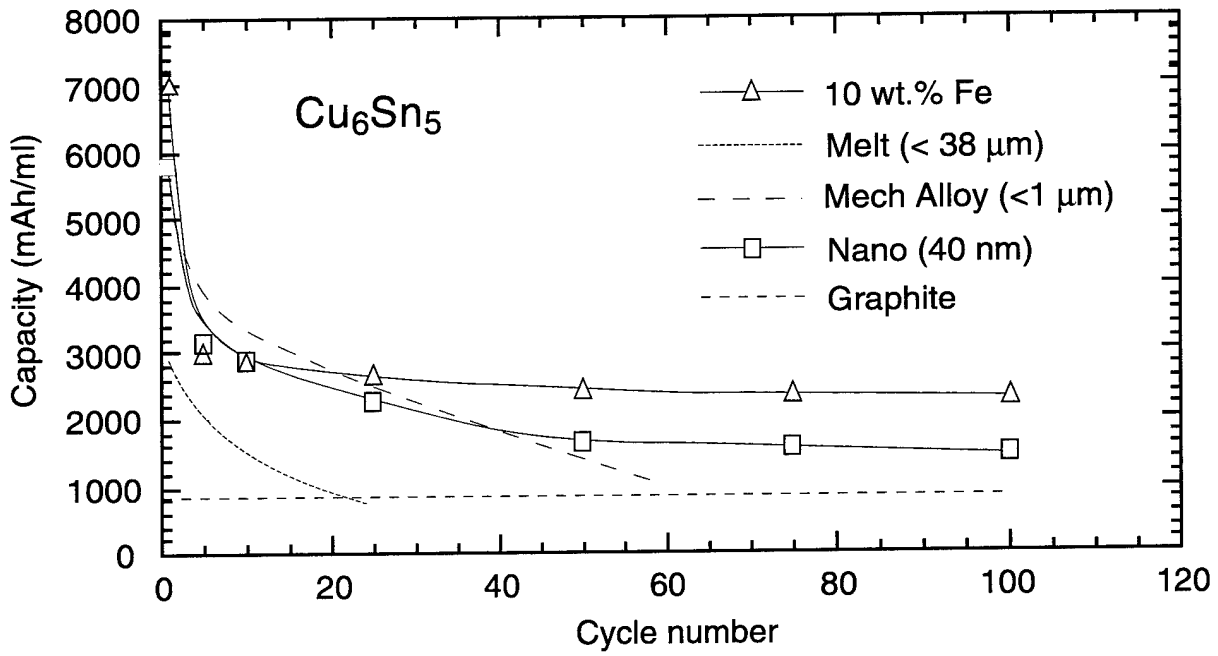

Figure 3. Volumetric Capacity Versus Cycle Number for the 10 Wt.% Fe, Nano-scale [15], Melted [12] and Mechanical Alloyed [14] Cu_6Sn_5 Materials Cycled in the Voltage Range 0.0–1.0 V (10 Wt.%Fe, nano-scale and melted) and 0.0–1.5 V (mechanical alloyed).

10 wt.% Fe material at 100 cycles is about 1.6 times the capacity that for the Cu_6Sn_5 alloy having nano-scale particles, even though the particle size is about 150 times larger (6 μm versus 40 nm). It is believed that this effect is a result of the increased resistance to fracture of grain boundaries in the Cu_6Sn_5 material containing Fe compared the Cu_6Sn_5 material without Fe. However, to confirm this suggestion, a very detailed analytical study would be required. Third, the volumetric capacity of the nano-scale Cu_6Sn_5 alloy at 100 cycles (≈1450 mAh/ml) is almost twice, while the capacity for Cu_6Sn_5-10 wt.% Fe material at 100 cycles (≈2320 mAh/ml) is almost three times the theoretical capacity of graphite (≈850 mAh/ml) [**11**]. Thus, both materials have potential as a replacement anode for graphite in Li-ion batteries.

It is therefore of interest to speculate what the capacity might be for the Cu_6Sn_5 alloy having both nano-scale particles and containing Fe. The gravometric capacity of the Cu_6Sn_5 alloy having nano-scale particles and with 10 Fe wt. % as function of Cu content (=55% Cu_6Sn_5) at 100 cycles is shown in Figure 4. The data are taken from Figure 3. The dotted line presents the theoretical capacity, assuming the following decomposition reaction:

$$4.4Li + Cu_ySn = yCu + Li_{4.4}Sn \quad (1)$$

From Figure 4, several important points are noted. First, as expected, as the amount of Cu decreases, the theoretical capacity decreases. Second, as shown earlier in Figure 3, the Fe has a greater effect of capacity retention than reducing the particle size to the nano-scale. Third, assuming that the impurity and particle size effects are independent, which is probably valid in a first approximation, it can be observed that in this case, the predicted capacity of a nano-scale particle size Cu_6Sn_5 alloy with the Fe addition will approach the theoretical value, assuming that the reversible capacity is associated with the decomposition of Cu_6Sn_5 to $Cu + Li_{4.4}Sn$. Thus, it is suggested that the use of a single method may not be sufficient and future work attempts to increase the cycle life of alloys should focus on the use of a combination of methods.

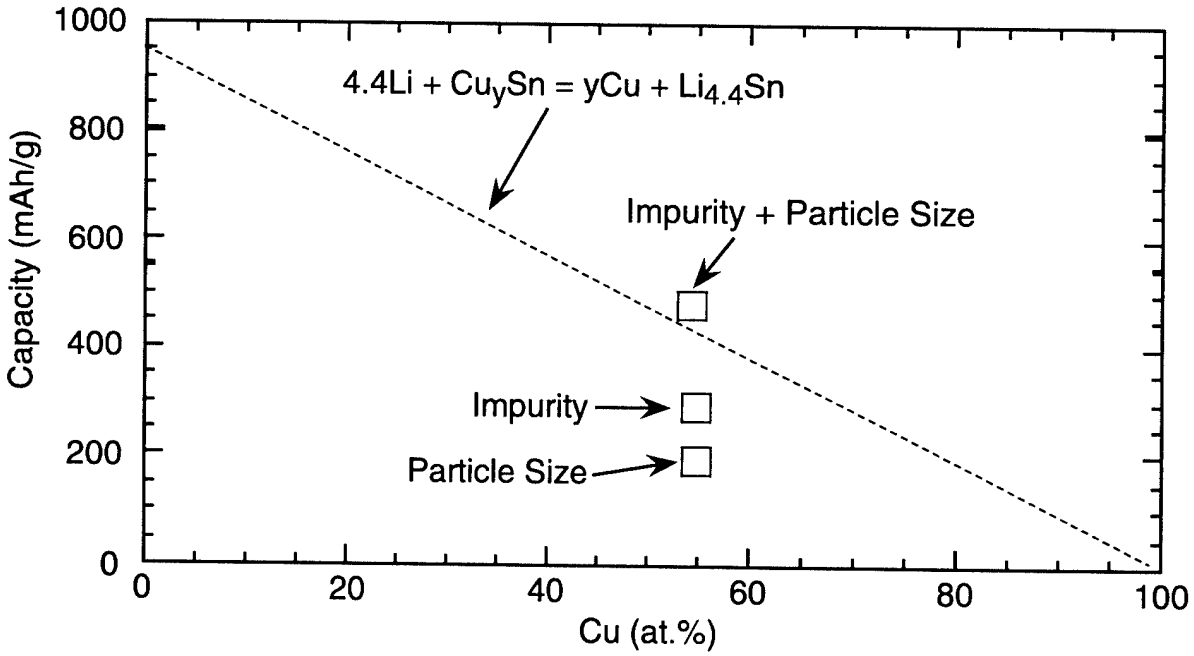

Figure 4. The Capacity of the Cu_6Sn_5 Alloy Having Nano-scale Particles (particle size) And/Or 10 Fe-wt. % (impurity) as Function of Cu Content (=55% Cu_6Sn_5) at 100 Cycles. (The dotted line represents the theoretical capacity for the decomposition of Cu_6Sn_5 to Cu + $Li_{4.4}Sn$.)

Conclusions

The results of this study can be summarized as follows:

1) Nano-scale Cu_6Sn_5 powders (< 100 nm) were synthesized by a chemical method that involved reduction of the metallic ions with a $NaBH_4$ solution.

2) An improvement in capacity retention can be obtained when the particle size of the Cu_6Sn_5 alloy was reduced from the micron to the nano-scale range. The volumetric capacity of the nano-scale Cu_6Sn_5 alloy at 100 cycles is almost twice the theoretical capacity of graphite.

3) A significant improvement in capacity retention of a Cu_6Sn_5 alloy was exhibited by the addition of 10-wt.% Fe compared to the alloy of similar particle size but without the Fe addition. It is believed that this effect is a result of the increased resistance to fracture of grain boundaries in the Cu_6Sn_5 material containing Fe compared the Cu_6Sn_5 material without Fe. The volumetric capacity of the Cu_6Sn_5 alloy containing Fe at 100 cycles is almost three times the theoretical capacity of graphite. Thus, the Cu_6Sn_5-10 wt.% Fe material has potential as a replacement anode for graphite in Li-ion batteries.

4) The Fe addition had a more significant effect on capacity retention than the reduction of the particle size to the nano-scale. For example, at 100 cycles, the reversible capacity is about 1.5 times higher for the Cu_6Sn_5 material containing Fe compared to the Cu_6Sn_5 material with the nano-scale particles.

5) If the impurity and particle size effects are independent, it can be expected that the predicted capacity of a nano-scale particle size Cu_6Sn_5 alloy with the Fe addition will approach the theoretical value, assuming that the reversible capacity is associated with the decomposition of Cu_6Sn_5 to Cu + $Li_{4.4}Sn$. Thus, it is suggested that the use of a single method may not be sufficient, and future work attempts to increase the cycle life of alloys should focus on the use of a combination of methods.

Acknowledgments

This work was performed under the Director's Research Initiative Program (FY01-SED-15) of the U. S. Army Research Laboratory.

References

1. M. Winter, J. O. Besenhard, *Electrochimica Acta* 45 (1999) 31.
2. O. Crosnier, X. Devaux, T. Brousse, P. Fragnanaud, D. M. Schleich, *J. Power Sources* 97-98 (2001) 188.
3. J. Wolfenstine, *J. Power Sources* 79 (1999) 111.
4. J. Yang, M. Wachtler, M. Winter, J. Besenhard, *Electrochem. Solid State Lett.* 2 (1999) 161.
5. O. Mao, R. L. Turner, I. A. Courtney, B. D. Fredericksen, M. I. Buckett, L. J. Krause, J. R. Dahn, *Electrochem. Solid State Lett.* 2 (1999) 3.
6. L. Fang, B. V. R. Chowdari, *J. Power Sources* 97-98 (2001) 181.
7. O. Crosnier, T. Brousse, X. Devaux, P. Fragnanud, D. M. Schleich, *J. Power Sources* 94 (2001) 169.
8. B. A. Boukamp, G. C. Lesh, R. A. Huggins, *J. Electrochem. Soc.* 128 (1981) 725.
9. G. X. Wang, L. Sun, D. H. Bradhurst, S. Zhong, S. X. Dou, H. K. Liu, *J. Power Sources* 88 (2000) 278.
10. C. Wang, A. J. Appleby, F. E. Little, *J. Power Sources* 93 (2001) 174.
11. K. D. Kepler, J. T. Vaughey, M. M. Thackeray, *Electrochem. Solid State Lett.* 2 (1999) 307.
12. K. D. Kepler, J. T. Vaughey, M. M. Thackeray, *J. Power Sources* 81-82 (1999) 383.
13. D. Larcher, L. Y. Beaulieu, D. D. MacNeil, J. R. Dahn, *J. Electrochem. Soc.* 147 (2000) 1658.
14. Y. Xia, T. Sakai, T. Fujieda, M. Wada, H. Yoshinaga, *J. Electrochem. Soc.* 148 (2001) A471.

15. J. Wolfenstine, S. Campos, D. Foster, J. Read, W. K. Behl, Journal of Power Sources, in press.
16. Y. Yamaguchi, U. Umakoghi, *Prog. Mater. Sci.* 34 (1990) 1.
17. D. B. Miracle, *Acta Metall. Mater.* 41 (1993) 649.
18. C. T. Liu, C. L. White, J. A. Horton, *Acta Metall. Mater.* 33 (1993) 649.
19. N. S. Stoloff, *Int. Mater. Rev.* 34 (1989) 153.
20. K. Masuda-Jino, *Mater. Sci.Eng. A* 192 (1995) 104.
21. J. A. Horton, M. K. Miller, *Acta Metall.* 35 (1987) 133,
22. C. A. P. Horton, *Scripta Metall.* 8 (1974) 1.
23. P. K. Chaudhury, K. T. Park, F. A. Mohamed, *Metall. Trans. A.* 25 (1994) 2391.
24. F. A. Mohamed, *Surf. Interface Anal.* 31 (2001) 532.
25. B. D. Cullity, *Elements of X-Ray Diffraction*, Addison-Wesley, Reading, MA, 1978.
26. M. I. Mendelson, *J. Am. Ceram. Soc.* 52 (1969) 443.

REPORT DOCUMENTATION PAGE

Form Approved
OMB No. 0704-0188

1. AGENCY USE ONLY *(Leave blank)*	2. REPORT DATE	3. REPORT TYPE AND DATES COVERED
	May 2002	Progress, Jan. 1, 2001 to Dec. 31, 2001

4. TITLE AND SUBTITLE Cycle Life Enhancement in Cu-Sn Anodes

5. FUNDING NUMBERS
DA PR: AH47
PE: 61102A

6. AUTHOR(S) Jeff Wolfenstine, Donald Foster, Jeffrey Read, and Wishvender Behl

7. PERFORMING ORGANIZATION NAME(S) AND ADDRESS(ES)
U.S. Army Research Laboratory
Attn: AMSRL-SE-DC email: jwolfenstine@arl.army.mil
2800 Powder Mill Road
Adelphi, MD 20783-1197

8. PERFORMING ORGANIZATION REPORT NUMBER
ARL-TR-2664

9. SPONSORING/MONITORING AGENCY NAME(S) AND ADDRESS(ES)
U.S. Army Research Laboratory
2800 Powder Mill Road
Adelphi, MD 20783-1197

10. SPONSORING/MONITORING AGENCY REPORT NUMBER

11. SUPPLEMENTARY NOTES
ARL PR: 1NENV1
AMS code: 611102.H4711

12a. DISTRIBUTION/AVAILABILITY STATEMENT Approved for public release; distribution unlimited.

12b. DISTRIBUTION CODE

13. ABSTRACT *(Maximum 200 words)*

This technical report summarizes the work on two different approaches that have been used to increase the cycle life of active-inactive composites in the copper-tin system. The first approach is to reduce the particle size of the active-inactive composities to the nano-scale (<100 nm). The second approach is the addition of extra elements that segregate to grain/phase boundaries and increase the cohesive strength of the boundary. Both approaches significantly improved the capacity retention of a Cu6Sn5 alloy. A larger improvement in capacity retention was exhibited by the addition of 10-wt.% iron compared to the reduction of the particle size to the nano-scale. The volumetric capacity of the Cu6Sn5 alloy containing 10 wt.% iron at 100 cycles is almost three times the theoretical capacity of graphite. The Cu6Sn5-10 wt.% Fe material has potential as a replacement anode for graphite in lithium-ion batteries.

14. SUBJECT TERMS	15. NUMBER OF PAGES
Anode, Li-ion, battery, capacity	14
	16. PRICE CODE

17. SECURITY CLASSIFICATION OF REPORT	18. SECURITY CLASSIFICATION OF THIS PAGE	19. SECURITY CLASSIFICATION OF ABSTRACT	20. LIMITATION OF ABSTRACT
Unclassified	Unclassified	Unclassified	UL

NSN 7540-01-280-5500

Standard Form 298 (Rev. 2-89)
Prescribed by ANSI Std. Z39-18
298-102